Regenerative Chatter Evaluation when Turning Nickel-based Superalloy GH4169 Using PCBN Cutting Tool

Mubarak A.M. Fadul Almula*[1,3], Haitao Zhu[2] & Hassan A. Wahab[3]

[1]College of Mechanical and Electrical Engineering, Harbin Engineering University, No.145 Nantong Street, Harbin 150001, China
[2]College of Ship Building Engineering, Harbin Engineering University, No. 145 Nantong Street, Harbin 150001, China
[3]Faculty of Engineering and Technical Studies, University of Elimam Elmahdi, Kosti, Sudan
*E-mail: mubarak092@gmail.com

Abstract. Vibration during machining operation is a major issue that lowers cutting operation efficiency. Usually high cutting forces are encountered during machining processes, consequently shortening cutting tool lifetime. Thus, the metal removable rate is reduced and a poor surface finish is produced. This issue can be overcome by selecting proper cutting parameters (cutting speed, feed, and depth of cut), especially when machining difficult-to-cut materials at high cutting speed. In this paper, a two-degrees-of-freedom turning vibration model is introduced to study the vibration mode of the system when nickel-based superalloy GH4169 is turned at varying cutting depths. The effect of varying the cutting depth on system vibration was simulated using the Matlab/Simulink software. In addition, the model was experimentally tested on a numerical controlled lathe machine. The stable limit cutting depth and the main vibration directions of the system chatter were the responses that were investigated. The results show that the simulation provided a reasonable approximation of the experimental results.

Keywords: *cutting depth limit of stability; high-speed cutting; nickel-based superalloy; PCBN cutting tools; regenerative chatter.*

1 Introduction

Nickel-base superalloy hard materials are widely used in many industrial applications due to their good structural, physical and chemical properties. However, they are hard to machine at high removable rate with minimum encountered process chatter. Usually, machining of such materials at improper cutting parameters (cutting speed, feed rate and cutting depth) results in high cutting forces. Consequently, high vibration is induced during the cutting process, which leads to a shorter tool lifetime and deleteriously affects the machined surface. Therefore, it is important to optimize these multi-objective cutting operations in order to achieve their highest possible efficiency. Presently, a sizeable amount of research is being conducted in increasing

Received November 10th, 2018, Revised March 29th, 2019, Accepted for publication August 6th, 2019.
 ISSN: 2337-5779, DOI: 10.5614/j.eng.technol.sci.2019.51.4.7

machining efficiency so that hard-to-cut materials can be machined at high removable rates with minimum possible process chatter [1,2]. Chatter during machining operations is usually generated by the internal excitation of the processing system. Over the past years, some research has been carried out to reduce chatter during cutting operations, including investigation of the cutting operations chatter mechanism, chatter monitoring and chatter suppression [3,4].

The outputs of these works can significantly help in the selection of the most effective method to improve cutting operation efficiency. They have revealed that choosing a highly rigid cutting tool and workpiece clamping play an important role in reducing machining chatter. In addition, they emphasize that the selection of the proper cutting conditions is considered the key solution towards eliminating or minimizing cutting process chatter. Hongwei, *et al.* [5] deduced the theoretical formula of the limit cutting width vs the change of the spindle speed for a single degree of freedom regenerative chatter system and thus established a stability limit prediction method for the cutting tool/machine system. Li, *et al*. [6] used a combination of a numerical simulation technique and experimental testing. They concluded that spindle speed, direction coefficient, coincidence degree and cutting stiffness during the turning operation significantly affect the limit cutting width value. Zhang, *et al*. [7] employed a Matlab/Simulink simulation to a two-degrees-of-freedom turning operation with which a chatter model was simulated and the limit cutting width was approximated. Huang, *et al.* [8] made a deep-cut test for 45 steel grades and found that machining chatter occurred at the natural frequency of the tool or of the workpiece. However, no experimental test was performed to verify the simulation results.

Regarding the machinability of nickel-based superalloy (GH4169), different research works have been performed when this material was turned using a variety of cutting tool materials. For instance, Nalbant, *et al.* [9] used a CVD coated cutting tool to study the effect of both cutting tool geometry and cutting speed on the cutting forces and surface roughness. Zhai, *et al*. [10] employed PVD-TiAlN coated carbide inserts to turn the GH4169 material at high speed. They investigated the influence of the cutting parameters on the surface integrity of the machined part using these different cutting tool materials. However, there is a lack of information in the reported literature about machining process stability when this hard nickel-based superalloy is turned using a PCBN cutting tool. Therefore, in this study, both simulation and experimental techniques were employed to investigate machining process stability when this nickel-based superalloy is turned with a PCBN cutting tool.

2 Materials and Methods

2.1 Turning Process Dynamic Model

The workpiece material used in this study was nickel-base superalloy GH4169. The workpiece diameter was 125 mm. The tailstock center was used as auxiliary support. Figure 1 shows the two-degrees-of-freedom dynamic model of the turning system, where the X and Y directions represent the longitudinal and radial feed directions, respectively. For convenience of analysis, the following simplifications were applied:

1. The workpiece system is more rigid than the tool holder and the cutting system is the main vibration system;
2. The system is vibrated linearly and the elastic restoring force of the vibrated system is proportional to the vibration displacement;
3. The damping force of the vibrated system is proportional to the vibration velocity;
4. The dynamic change of cutting thickness is influenced by the regeneration effect;
5. The feed direction of the cutting tool has two degrees of freedom.

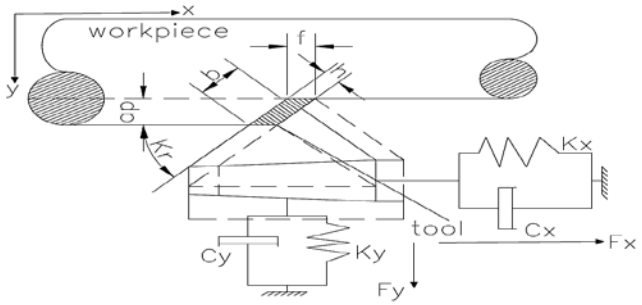

Figure 1 Two-degrees-of-freedom cylindrical turning chatter model.

According to the kinetics of the model shown in Figure 1, the equations of motion in the X and Y directions are expressed by Eqs. (1) and (2) respectively:

$$\text{X-direction: } F_x(t) = m_x\ddot{x}(t) + c_x\dot{x}(t) + k_x x(t) \tag{1}$$

$$\text{Y-direction: } F_y(t) = m_y\ddot{y}(t) + c_y\dot{y}(t) + k_y y(t) \tag{2}$$

where *Fx(t), Fy(t)* are the dynamic cutting forces of the vibrated system in the X and Y directions given in (N); m_x, m_y are the equivalent masses of the main vibrated system in the X and Y directions and given in (g); the equivalent masses (m_x, m_y) were calculated using the relationship between the stiffness coefficient and the frequency ($k/\omega n^2$) in the X and Y directions, respectively; c_x

and c_y represent the equivalent damping coefficients of the main vibrated system in the X and Y directions and are given in (N.s /mm); k_x and k_y are the equivalent stiffness coefficients of the main vibrated system in the X and Y directions and are given in (N/mm).

The components of the resultant dynamic cutting forces are given by Eqs. (3) and (4):

$$F_x(t) = k_c bh(t) \tag{3}$$

$$F_y(t) = k_e bh(t) \tag{4}$$

where k_c, k_e are the cutting stiffness coefficients of the main vibrated system in the X and Y directions given in (N /mm^2); b is the cutting width (mm); and $h(t)$ is the dynamic cutting thickness (mm).

The dynamic cutting thickness can be expressed as in Eq. (5):

$$h(t) = f \sin k_r + \Delta x \sin k_r - \Delta y \cos k_r \tag{5}$$

where f is the feed rate in (mm/rev), k_r is the side cutting edge angle of the tool, Δx,Δy are the differences between the vibration displacement in the X and Y directions and are given in (mm).

Δx and Δy can be determined by Eqs. (6) and (7):

$$\Delta x = \mu x(t-T) - x(t) \tag{6}$$

$$\Delta y = \mu y(t-T) - y(t) \tag{7}$$

where [$x(t\text{-}T)$ - $x(t)$] is the dynamic chip thickness due to the tool vibration; $y(t\text{-}T)$ is the displacement of the tool during the previous pass; and $y(t)$ is the vibration displacement of the tool; μ is the overlap factor in the successive cuts; T is the time duration of one full rotation of the workpiece; N is the spindle speed in (rev/min). According to the kinetic model shown in Figure 1, the system equations of motion can be obtained as follows:

$$k_c bh(t) = m_x \ddot{x}(t) + c_x \dot{x}(t) + k_x x(t) \tag{8}$$

$$k_e bh(t) = m_y \ddot{y}(t) + c_y \dot{y}(t) + k_y y(t) \tag{9}$$

The vibrational displacement of the system can be expressed as in Eq. (10):

$$y(t) = A\sin(\omega t) \tag{10}$$

where *A* is the amplitude in (mm), ω is the angular frequency of vibration in (rad/s), [11]. Based on the above dynamic model (equations of motion) and using Laplace transformation, the maximum cutting width in the X and Y directions can be given by Eqs. (11) and (12) respectively:

$$b_{lim,x} = \frac{-2\zeta_x \lambda_x k_x}{k_c \zeta sin\left[arcsin \frac{2\zeta_x \lambda_x}{\sqrt{(2\zeta_x \lambda_x)^2 + (1-\lambda_x{}^2)^2}} - arctan \frac{2\zeta_x \lambda_x}{1-\lambda_x{}^2} \right]} \tag{11}$$

$$b_{lim,y} = \frac{-2\zeta_y \lambda_y k_y}{k_e \zeta sin\left[arcsin \frac{2\zeta_y \lambda_y}{\sqrt{(2\zeta_y \lambda_y)^2 + (1-\lambda_y{}^2)^2}} - arctan \frac{2\zeta_y \lambda_y}{1-\lambda_y{}^2} \right]} \tag{12}$$

where b_{limx}, b_{limy} are the directional limit cutting widths; ζx and ζy are the damping ratios of the system; λ_x and λ_y are the frequency ratios in the X and Y directions. λ_x is equal to $\omega / \omega n_x$ and λy is equal to $\omega / \omega n_y$ where ω is the frequency of the vibration angle and ωn_x, ωn_y are the natural frequencies of the system in the X and Y directions.

2.2 Model Parameters

The above regenerative chatter model represents a two-degrees-of-freedom turning operation. The ultimate cutting width was calculated using the measured natural frequency ω, damping ratio ζ and stiffness K of the system. The above parameters of the model were measured using the hammering measuring method. The measurements were performed using simple Kistler 9722A500 hammers, which are considered convenient for testing turning operations [12]. The acceleration sensor for the signal sampling in the X and Y directions and their installing locations are shown in Figures 2(a) and (b).

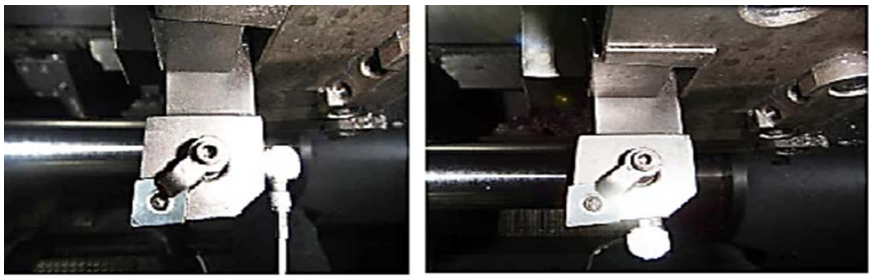

(a) (b)

Figure 2 (a) Installation of the acceleration sensor in the X direction, (b) installation of the acceleration sensor in the Y direction.

The sampling frequency was 5000 Hz. The sample data were analyzed and the directional frequency response function (FRF) in the X and Y directions was calculated by the (HRsoft (MA) V1. 9) software (Figures 3 and 4). The measured values of the modal parameters are tabulated in Table 1.

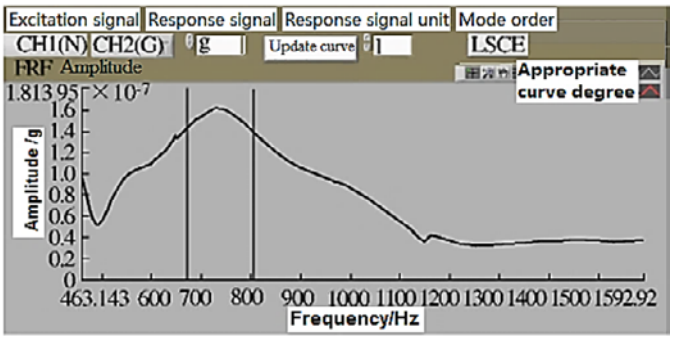

Figure 3 The frequency response function in the X direction.

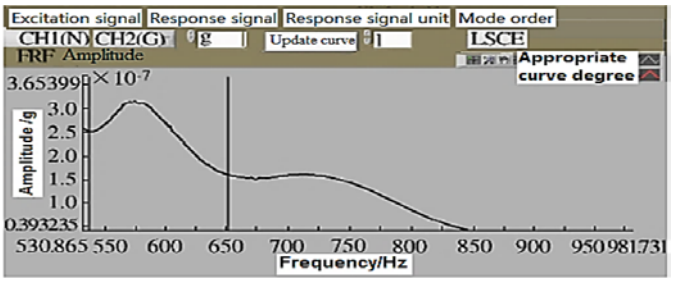

Figure 4 The frequency response function in the Y direction.

The acceleration sensor for the signal sampling in the X and Y directions and their installing locations are shown in Figures 2(a) and (b). The sampling frequency was 5000 Hz. The sample data were analyzed and the directional frequency response function (FRF) in the X and Y directions was calculated by the (HRsoft (MA) V1. 9) software (Figures 3 and 4). The measured values of the modal parameters are tabulated in Table 1.

Table 1 Measured modal parameters in the X and Y directions.

Direction	Modal frequency /Hz	Modal Damping /%	Modal Stiffness /N/m	Modal Mass /kg
X	721.64	4.87	$6.39*10^7$	122.70
Y	565.96	3.12	$5.23*10^7$	162.94

2.3 Simulation Block Diagram

The chatter model was designed according to two-dimensional cylindrical turning using the measured modal parameters as shown in Figure 5. Then the Matlab/Simulink software was used to simulate the model. The simulation was carried out in both the X and the Y direction.

Two spring damping systems and an encapsulated subsystem called Subsystem1 were identified. The simulation model of the input port included feed rate, spindle speed, back cutting depth, and three manual input modules. The output port included two output modules; these were the tool point and the vibration displacement in the X and Y directions, which were varied with time.

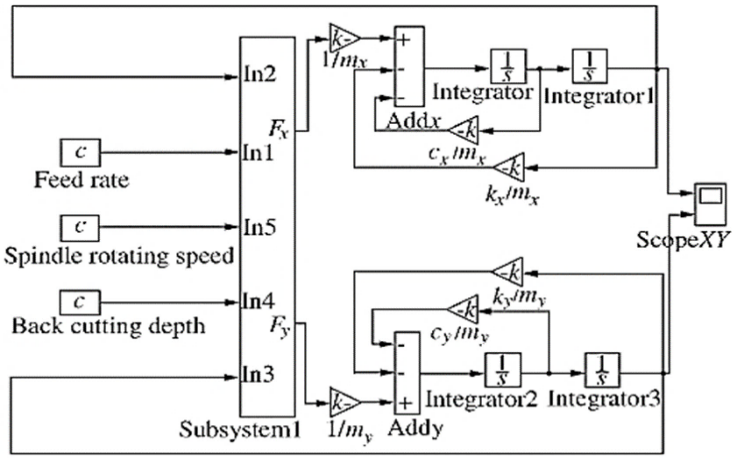

Figure 5 Simulation block diagram of cylindrical turning chatter.

Subsystem1 is a packaged subsystem module and its internal structure is shown in Figure 6. Subsystem1 is the input port of subsystems (In_1) to In_5. (In_1) is the input port of the feed rate value. (In_2) represents the input port of the vibration displacement in the X direction. Port (In_3) is assigned for inserting the input vibration displacement in the Y direction, while ports (In_4 and In_5) are the input ports for back cutting depth and spindle rotating speed, respectively.

Fx and Fy are the output ports for the subsystem, which are the dynamic cutting forces in the X and Y directions, while ($System_2$) to ($System_8$) are the inputs and multi-outputs conversion modules of the signal shunting. Product1 to Product6" are the multiplier modules, which were used for multiplying the signals. Kc and Ke are the proportional modules in the diagram. The average unit cutting force coefficients were assigned to the X and Y directions.

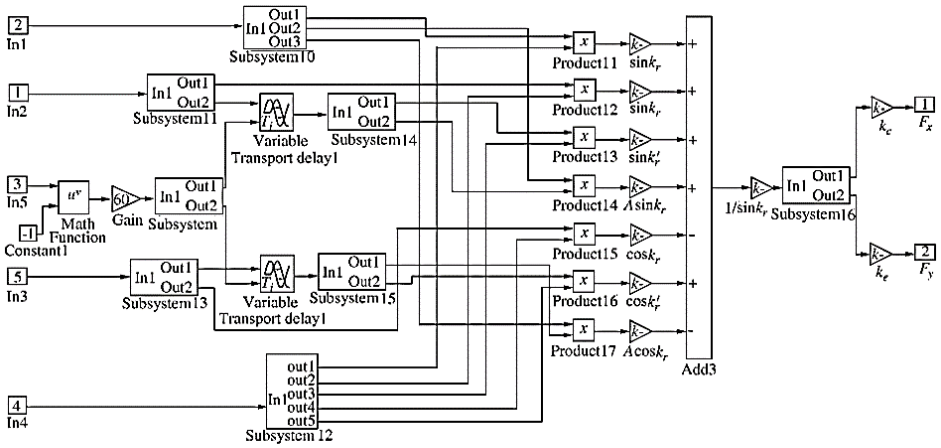

Figure 6 The block diagram of Subsystem1.

After the workpiece had been treated with a solid solution or aging treatment, the cutting force in the cutting area of the nickel-base superalloy material was found to be 4150 N /mm^2 [10]. According to the principles of cutting movement in orthogonal turning, the average angle of axial, radial and cutting forces can easily be determined. Thus, the average cutting force coefficient in the X and Y directions was calculated by a trigonometric function.

Therefore, the regenerative effect of chatter for this module was evaluated using the Subsystem1 diagram. On the other hand, coincidence degree μ, which changes with the feed and depth of the cut, can be calculated using the following equation:

$$\mu = \frac{\sin k_r \sin k_r'}{\sin(k_r + k_r')} \times \frac{f}{a_p} \tag{13}$$

Kr and k'r are the side cutting edge and end cutting edge angles of the tool, which depend on the tested tool type (Figure 7) According to Eq. (13), the coincidence degree has a direct effect on regeneration chatter. Therefore, simulation of the model was performed using a variable step size algorithm, where the program type selects the variable-step and the solver (simulation algorithm), which was ode45 (Dormand-Prince). In addition, all the initial values of the integrator module were set to zero. The measured modal parameters were the main input values. The other parametera used in this simulation were the side cutting edge angle, which was equal to 0°; the end cutting edge angle, which was equal to 5° to avoid interference between the machined surface and the tool; the side rake angle was 0°; the back rake angle was 0°, Kc = 1010 MPa and Ke = 1377 MPa.

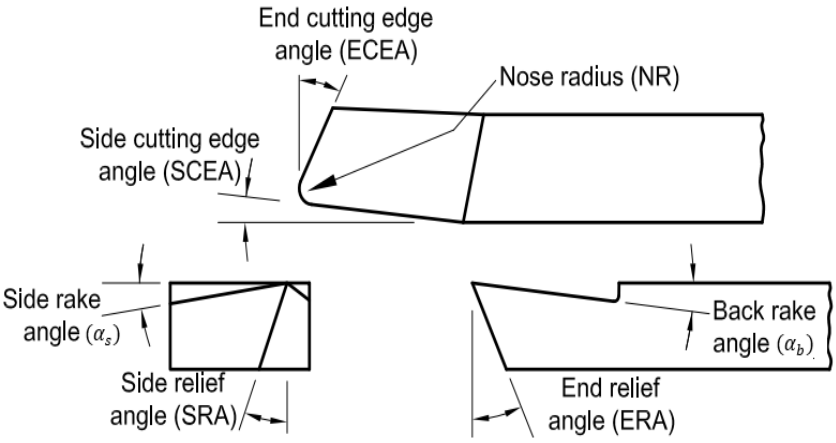

Figure 7 The angles of a single-point cutting tool.

3 Results and Discussion

3.1 Simulation

The simulation was carried out at constant cutting speed (80 m/min) and feed (0.15 mm/rev) while the depth of the cut was varied at four levels (1.5 mm, 1.98 mm, 2.5 mm, and 4.56 mm). The tool vibration in the X and Y directions at a cutting depth of 1.5 mm is shown in Figure 8(a).

In this case, the system is in a stable cutting state. However, when the cutting depth reaches 1.98 mm, the tool vibration in the X direction is attenuated, while the amplitude in the Y direction is almost constant and is in a critical divergent state (Figure 8(b)). Therefore, this value of the depth of cut (1.98 mm) was taken as the limit cutting depth in the Y direction.

When the cutting depth continues to increase to 2.5 mm, the amplitude of the tool in the X and Y directions increases and thus the vibration is enhanced (Figure 8(c)). Hence, the tool vibration in the X direction is in a convergent state, while in the Y direction it tends to diverge to unstable cutting state.

When the cutting depth continues to increase to 4.56 mm, the vibration in the X direction tends to diverge up to unstable cutting condition (Figure 8(d)). It is concluded that the tool system first reaches unstable state in the Y direction and then with increasing depth of cut it reaches unstable state in the X direction.

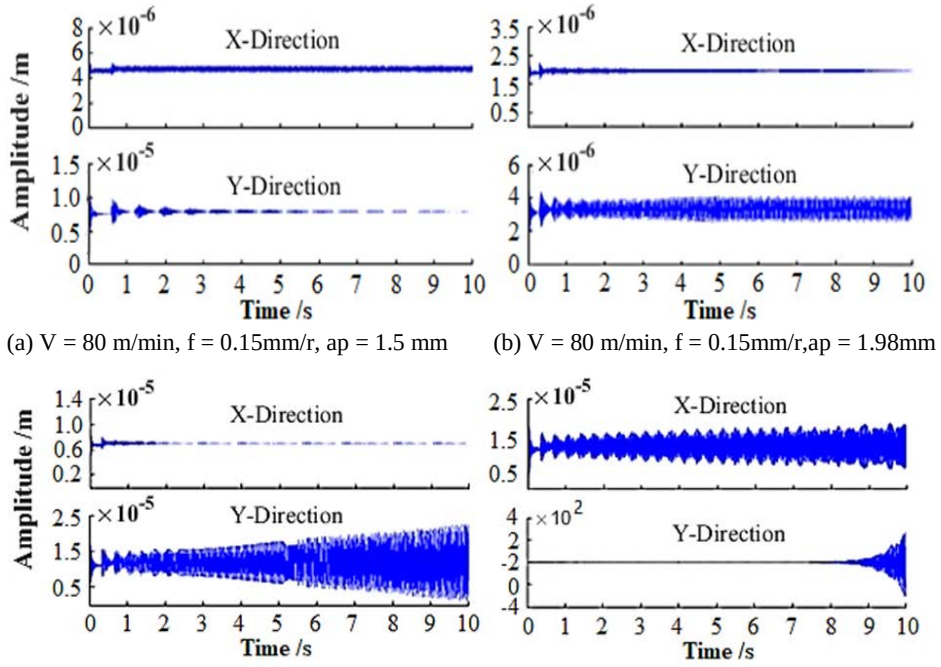

(a) V = 80 m/min, f = 0.15mm/r, ap = 1.5 mm (b) V = 80 m/min, f = 0.15mm/r,ap = 1.98mm

(c) V = 80 m/min, f = 0.15 mm/r, ap = 2.5 mm (d) V = 80 m/min, f = 0.15mm/r,ap = 4.56mm

Figure 8 Vibration time diagram of X and Y under different cutting parameters.

3.2 Turning Test

A cutting test on samples of a nickel alloy rod GH4169 with a diameter of 125 mm was carried out on (Seiko HTMTC40) CNC lathe machine (Figure 9). The test was performed with a varied depth of cut to assess the vibration of the cutting tool system (Figure 10).

The cutting tool designation used in this test was a CNGA120408 type 2, PCBN blade on an MCLNL type tool holder. The cutting trails were excircle dry turning. The vibration signals from the cutter were collected using a (Kistler 8765A250M5) three acceleration sensors with a sampling frequency of 5000 Hz.

The workpiece was turned into a cone with a cone angle of 20° at varied cutting depths, while the cutting speed and the insertion speed were maintained at invariant quantities. When the cutting depth reached the limit cutting depth, the system vibration suddenly increased, leaving a tool mark on the workpiece surface and at this stage the cutting process was stopped.

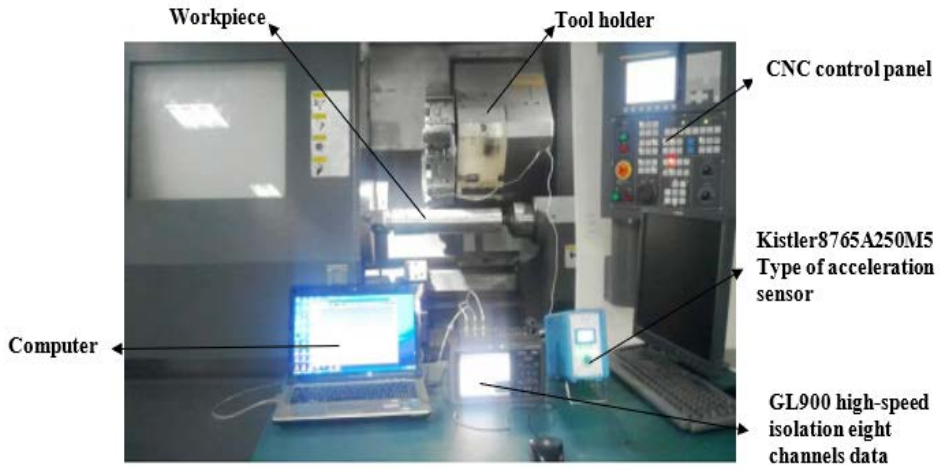

Figure 9 Set-up of turning test.

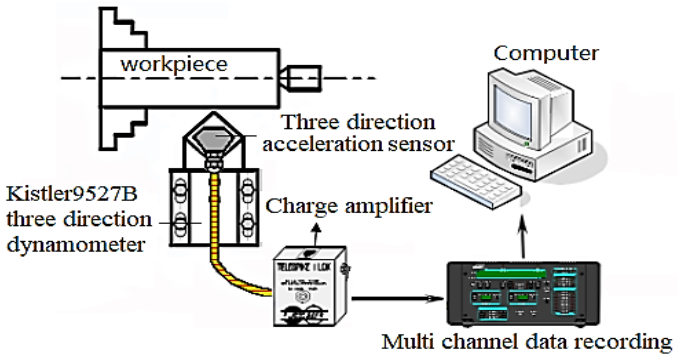

Figure 10 Schematic diagram of vibration monitoring.

The cutting parameters employed during this test were: cutting speed v = 80 m/min, initial cutting depth ap0 = 0.1 mm. The feed was selected to be as small as 0.15 mm/rev in order to increase the effect of regenerative vibration due to the increase of cutting depth. At the end of the experiment, the distance from the feed rate to the vibrating mark was measured by L_{lim}, and the side cutting edge angle of the tool in the experiment kr = 0°, and $b_{lim} \approx ap_{lim}$ were used.

According to Figure 11, the equation for calculating the limit cutting depth is:

$$a_{plim} = L_{lim} \bullet tan10^{o} + 0.1 \tag{14}$$

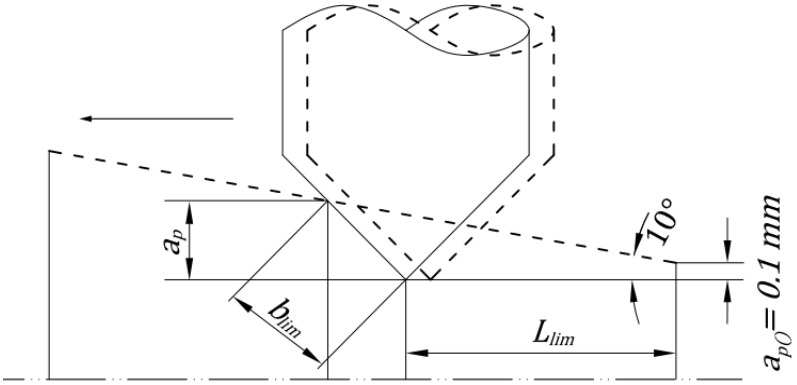

Figure 11 Schematic diagram of the cutting depth method.

Figure 12 shows the vibration time-domain diagram in the X and Y directions. It can be observed that at the beginning of the cutting action, the amplitude increases steadily with the increase of the cutting depth. When the cutting action is continued to 25 s the amplitudes of X and Y suddenly increase, and the vibration in the Y direction is remarkably stronger than that in the X direction. This vibration is accompanied by the tool scratching lines on the machined surface of the workpiece as shown in Figure 13.

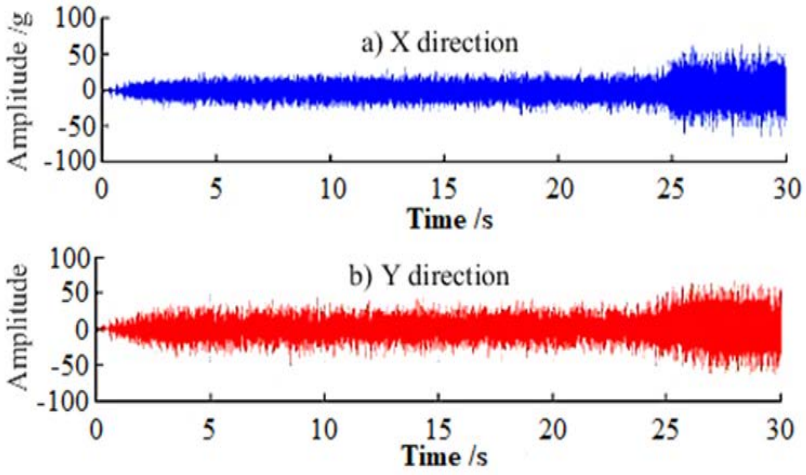

Figure 12 The time-domain waveform of the X and Y directions.

Figure 13 Chatter marks.

Therefore, in order to study the change of the vibration amplitude and the frequency during the cutting process, data were processed at 5 s, 15 s, and 25 s. These values were selected to view the samples at three different cutting durations. The time-vibration frequency plots of 5 s and 15 s in the X and Y directions are shown in Figures 14 and 15 respectively.

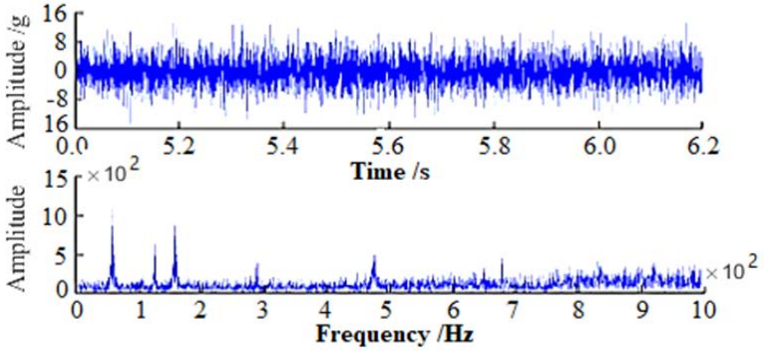

(a) X-direction

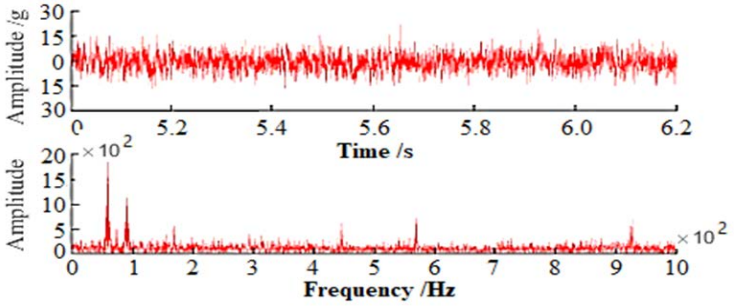

(b) Y-direction

Figure 14 Time-frequency diagram of vibration in the X and Y directions at 5 s.

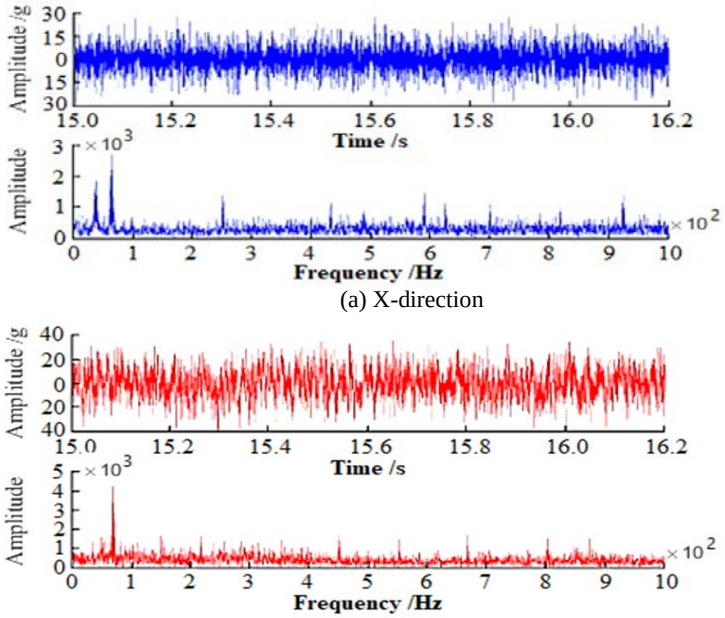

(a) X-direction

(b) Y-direction

Figure 15 Time-frequency diagram of vibration in the X and Y directions at 15 s.

The experimental results show that the amplitude of X and Y increased gradually with the increase of cutting depth before 25 s. It was observed that the vibration degree in the Y direction was larger than that in the X direction. During this period, although there were peaks that appeared in the frequency domain, they were concentrated in the low-frequency range, i.e. below 100 Hz (Figure 16). In addition, it was observed that the overall frequency distribution was more uniform, which indicates that the forced vibration prevailing system was in a stable cutting state. Thus, the amplitude of the vibration signals in the X and Y directions obviously increased and the degree of dispersion was higher.

It can be concluded that when cutting action continues to 25 s, the amplitude in the X and Y directions continues to increase and the degree of dispersion increases significantly. Although the degree of vibration in the X direction is exacerbated, there is no energy concentration in the frequency domain. However, the energy in the Y direction is mainly concentrated at a frequency range of about 538 Hz.

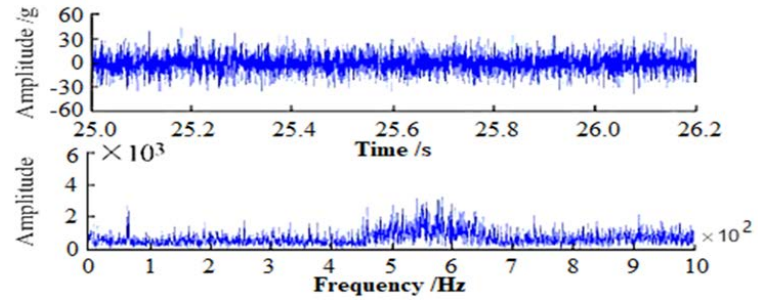

(a) X-direction

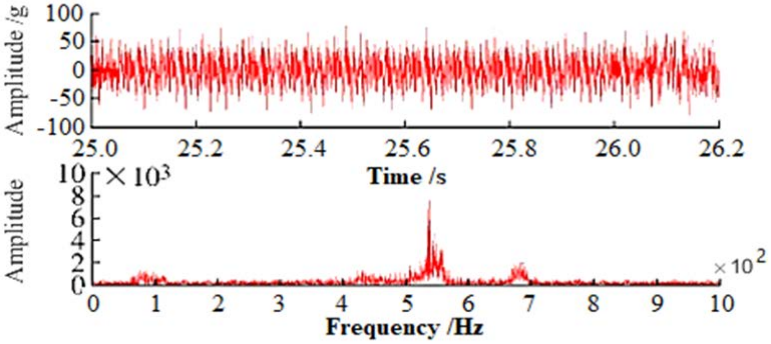

(b) Y-direction

Figure 16 Time-frequency diagram of vibration in the X and Y directions at 25 s.

In this case, the frequency structure tended to be noticeable, so the vibration mode of the system had changed from forced vibration to transition and from forced vibration to intensive self-excited vibration, achieving an unstable cutting state. In summary, the measured values of L_{lim} and ap_{lim} were found to be 12.88 mm and 2.37 mm respectively. Comparing with the results obtained from the simulation, the error rate of the limit cutting depth was:

$$\frac{2.37-1.98}{2.37}=16.45\%$$

4 Conclusions

The predicted limit cutting depth of two-degrees-of-freedom turning regenerative chatter is 1.98 mm. Compared with the measured limit cutting depth from the experiment, the error was found to be 16.45%. Therefore, the simulation result of the regenerative chatter model is accurate and effective.

The frequency of the cutting chatter was 538 Hz, which is close to the natural frequency of 565 Hz of the cutting tool system in the Y direction. This indicates that when the stiffness and quality of the workpiece system are much higher than those of the cutting tool system, the system vibration of the tool is reasonable.

Both the simulation and the cutting experiments showed that with increasing cutting depth, the tool system first achieves an unstable cutting state in the Y direction. Therefore, the Y direction was the main vibration direction of the cutting chatter found in this study.

Acknowledgment

This paper was funded by the international exchange program of Harbin Engineering University for Innovation-oriented Talented Cultivation.

References

[1] Ertürk, A., Özgüven, H.N. & Budak, E., *Analytical Modeling of Spindle-tool Dynamics on Machine Tools Using Timoshenko Beam Model and Receptance Coupling for the Prediction of Tool Point FRF*, Int. J. Mach. Tools Manuf, **46**(15), pp. 1901-1912, 2006.

[2] Liu, J., Cao, J., Lin, X., Song, X. & Feng, J., *Microstructure and Mechanical Properties of Diffusion Bonded Single Crystal to Polycrystalline Ni-Based Superalloys Joint*, Mater. Des., **49**, pp. 622-626, 2013.

[3] Thompson, R.A., *On the Doubly Regenerative Stability of a Grinder: the Effect of Contact Stiffness and Wave Filtering*, J. Eng. Ind., **114**(1), pp. 53-60, 1992.

[4] J. Gradišek., *On Stability Prediction for Milling*, Int. J. Mach. Tools Manuf, **45**(7), pp. 769-781, 2005.

[5] Hong-wei, Z., Xiao-jun, W. & Jun-yi, Y., *Prediction of Stability Limits For Regenerative Chatter System of Machine Tools*, J. Southwest Jiaotong Univ., **38**(5), pp. 547-554, 2003.

[6] Li, J., Xie, H., Sheng, Z. & Liu, Y., *Modeling and Simulation of Regenerative Chatter Stability in CNC Lathing Process*, J. Northeast. Univ. Natural Sci., **1**, pp. 29, 2013.

[7] Zhang, Y., He, Y. & Chen, X., *Simulation Analysis on the Cylindrical Turning Based on MATLAB/Simulink* , Mech. Res. Appl., **2**, pp. 11, 2013.

[8] Huang, Q., Zhang, G.B., Zhang, X.Y. & Cao, D., Experimental Analysis on Regenerative Chatter Model, J. Vib. Eng., **21**(6), pp. 547-552, 2008.

[9] Nalbant, M., Altin, A. & Gökkaya, H., *The Effect of Coating Material And Geometry of Cutting Tool and Cutting Speed on Machinability*

Properties of Inconel 718 Super Alloys, Mater. Des., **28**(5), pp. 1719-1724, 2007.

[10] Zhai, Y.S., Qiao, S., Liu, X.L. & Hu, Q., *The Simulation Analysis and Experimental Research on the Process of PCBN Cutting Super-Alloy*, Key Engineering Materials, **589**, pp. 88-93, 2014.

[11] Wang, X.J., *Study on the Prediction of Stability Limits in Turning*, Doctoral Dissertation, Shandong University of Technology, Shandong, Zibo, Zhangdian, China, pp. 20-39, 2005.

[12] Pawade, R.S., Joshi, S.S. & Brahmankar, P.K., *Effect of Machining Parameters and Cutting Edge Geometry on Surface Integrity of High-Speed Turned Inconel 718*, Int. J. Mach. Tools Manuf., **48**(1), pp. 15-28, 2008.